# Facile Chemical Growth of $Cu(OH)_2$ Thin Film Electrodes for High Performance Supercapacitors

# 간단한 화학적 합성을 통한 고성능 슈퍼캐패시터용 수산화 구리 전극

U. M. Patil, Min Sik Nam, N. M. Shinde, Seong Chan Jun†
U. M. Patil, 남민식, N. M. Shinde, 전성찬†

*Nano ElectroMechanical Device Laboratory, School of Mechanical Engineering, Yonsei University, Seoul 120-749, Korea.*
*† E-mail:scj@yonsei.ac.kr; Fax: +82-2-312-2159; Tel: +82-2-2123-5817*

**Abstract**

본 연구에서는 간단한 화학적 합성 방법을 통하여 스테인레스 기판 위에 nano-bud 형태의 수산화 구리 박막을 형성하였다. 그리고 또 다른 합성 방법인 chemical bath deposition을 이용하여 수산화 구리 나노 구조를 간단하고 친환경적으로 형성하였다. 수산화 구리 박막의 구조적 연구는 X-ray diffraction (XRD), X-ray photoelectron spectroscopy (XPS), field emission scanning electron microscopy (FESEM) 방법을 통하여 이루어졌으며 다결정의 nano-bud 형상을 확인할 수 있었다. 또한 나노 구조로 합성된 수산화구리 전극의 전기화학적 측정은 1M KOH의 전해질 조건에서 cyclic voltammetry (CV) and galvanostatic charge-discharge (GCD)에서 측정되었으며 340 F $g^{-1}$의 높은 비 용량을 보였다. 또한 1 mA $cm^{-2}$ 의 전력 밀도에서 ~83 Wh $kg^{-1}$의 높은 에너지 밀도와 ~3.1 kW $kg^{-1}$의 높은 출력 밀도를 가지며 향상된 전극의 성능을 보였다. 이러한 뛰어난 의사 캐패시터의 성능은 수산화 구리의 nano-bud 형상에 의한 효과로 확인할 수 있었다. 본 연구를 통하여 화학적 합성 방법의 확장을 통하여 수산화 구리 전극의 에너지 저장 장치로써의 성능을 확인할 수 있었다.

A facile soft chemical synthesis route is used to grow nano-buds of copper hydroxide [$Cu(OH)_2$] thin films on stainless steel substrate[SS]. Besides different chemical methods for synthesis of $Cu(OH)_2$ nanostructure, the chemical bath deposition (CBD) is attractive for its simplicity and environment friendly condition. The structural, morphological, and electro-chemical properties of $Cu(OH)_2$ thin films are studied by means of X-ray diffraction (XRD), X-ray photoelectron spectroscopy (XPS), field emission scanning electron microscopy (FESEM), cyclic voltammetry (CV) and galvanostatic charge-discharge (GCD) measurement techniques. The results showed that, facile chemical synthesis route allows to form the polycrystalline, granular nano-buds of $Cu(OH)_2$ thin films. The electrochemical properties of $Cu(OH)_2$ thin films are studied in an aqueous 1 M KOH electrolyte using cyclic voltammetry. The sample exhibited supercapacitive behavior with 340 F $g^{-1}$ specific capacitance. Moreover, electrochemical capacitive measurements of $Cu(OH)_2$/SS electrode exhibit a high specific energy and power density about ~83 Wh $kg^{-1}$ and ~3.1 kW $kg^{-1}$, respectively, at 1 mA $cm^{-2}$ current density. The superior electrochemical properties of copper hydroxide ($Cu(OH)_2$/SS) electrode with nano-buds like structure mutually improves pseudocapacitive performance. This work evokes scalable chemical synthesis with the enhanced supercapacitive performance of $Cu(OH)_2$/SS electrode in energy storage devices.

*Keywords: $Cu(OH)_2$, Chemical Bath Deposition, Granular Nano-buds, Supercapacitor,*

## I. INTRODUCTION

Supercapacitors are the intermediate energy storage device that can deliver much higher power densities than conventional batteries and higher energy densities than traditional capacitors. They can be charged and discharged at high rates with long cycle life and low maintenance cost. Supercapacitors can be divided into two types, based on the mechanism of the charge storage, pseudocapacitor and electric double layer capacitor (EDLC) [1]. In EDLC the charges are stored at the electrode/electrolyte interface, while for pseudocapacitors the charges are generated within the electrode due to a faradic reaction. Since the charges in EDLC are stored at the electrode surface, they are readily accessible and resulting in high power densities. In contrast, pseudocapacitive-type materials generate large number of charges due to redox reactions; deliver high energy density than that of carbonaceous materials which store charges only at the electrode surface by EDLCs [2,3]. Generally, metal hydroxides/ oxides and conductive polymers with multiple oxidation states, which possess a redox reaction, are used as pseudocapacitive materials [4].

In current years, the research aim in finding novel materials progressively changing from conventional intercalation chemistry to conversion based mechanisms. Studies in this manner are principally focused on diverse transition metal oxides/hydroxide due to their large capacities, through phenomenon of electrochemistry based redox reaction. In accordance with high specific capacity, the conversion reactions in transition metal oxides/hydroxides accompanying volume expansion upon long cycling, results into capacity diminution. However, some excellent performances have been achieved with metal oxides/hydroxides by evolving morphology advancement

ISSN 2465-8111 DOI http://dx.doi.org/10.18770/KEPCO.2015.01.01.175

to various hierarchical porous nanostructures [1]-[3]. Regrettably, the transition metal oxides based anodes suffer from capacity fading and poor cycling performance due to substantial structural and volume changes cause severe electrode pulverization arising while charge/discharge processes. This mechanical transfusion is main obstruction which inhibits their use in commercial application. Therefore, it is challenging to improve long cycle life with high capacities in transition-metal oxides to fulfill emerging future demands of anode materials in energy storage [2]-[4]. It is important for pseudocapacitor materials to have high specific surface area, high electrical conductivity and fast charge diffusion process in order to achieve high power and energy densities. Hydrous ruthenium oxides with amorphous structure have been reported to be promising electrode materials for pseudocapacitors applications due to their intrinsically excellent quasi-metallic conductivity and high pseudocapacitance. However, high cost and toxic nature of the compound has placed huge obstacles for its large scale manufacture. Therefore, a lot of effort has been devoted to develop alternative pseudocapacitor electrode materials such as NiO, $MnO_2$ and CuO [5][6].

Among these transition metal oxides, CuO, is an important p-type semiconductor having a narrow band gap ($E_g$=1.2 eV). It is promising in various fields of application such as, a potential field emission material, catalyst, a gas-sensing medium, in making optical switches and solar cells due to its photoconductive and photochemical properties [5][6]. CuO has high specific capacity (670 mA h $g^{-1}$) hence considered as efficient anode material with merits such as, resource abundance, economic, non-toxic, easy production, and environmental friendliness [6]. Copper oxide (CuO) is one of the suitable metal oxides with favorable pseudo-capacitive properties, and thus CuO thin films synthesized by electrodeposition [5] and chemical bath deposition (CBD) [6] have been used in supercapacitors. However, highest specific capacitance is limited to 37 and 43 F $g^{-1}$, respectively. The minor enhancement in the supercapacitance performance of CuO has been achieved by either forming hybrid films (CuO/PPA) [7] or composite with CNTs [8], in which the specific capacitance is limited to 65 and 60 F $g^{-1}$, respectively. In spite of these merits, due to poor electrical conductivity it also suffers loss of capacity upon cycling. Many efforts have been taken to increase the electrochemical performance of CuO materials. To resolve these difficulties, many researchers aimed their efforts in performance advancement by growing various micro-nanostructures, morphologies and hybrid composite materials with boosting electrochemical properties and unique structures [8].

Recent studies demonstrate that metal hydroxides exhibit higher specific capacitance than metal oxides counterparts [9][10]. Thus, current studies have been focused on synthesis of metal hydroxide thin films. Among many metal oxides/hydroxides, $Cu(OH)_2$ is advantageous in terms of low cost and abundance in nature; therefore, it is considered a promising lucrative pseudocapacitive material in supercapacitors. There are few reports available on preparation of $Cu(OH)_2$ by chemical (precipitation, SILAR, Sol-gel, hydrothermal, etc) and electrochemical deposition (ED) methods for its application in supercapacitors [11][12]. It is noteworthy that, for total capacitance only surface part of electro-active material in contact with the electrolyte can majorly contribute in the redox reactions for energy storage. Hence, smart engineering of electrode material is highly required. The directly growing smart multifarious nanostructures of metal hydroxides on conducting substrates are constructive for supercapacitors. Such a binder free electrode is more feasible offering fast electron-transport, easy electrolyte diffusion with more access of electro-active sites by sinking weight and resistance of material. Thus, synergetic characteristics can be instantaneously attained for improving specific capacitance, stability and rate performance of electrode components [13]. So, chemical bath deposition (CBD) can be facile method for $Cu(OH)_2$ preparation. Chemical bath deposition method offers many advantages over other deposition methods such as, low temperature, any complex shaped conducting substrates can be used and morphology can be easily controlled by deposition parameters such as temperature, complexing agent. Furthermore, this method is simple and possesses the potential for large-area deposition. Still, there are only few reports are available on the synthesis of $Cu(OH)_2$ on Ni foam and different kinds of metal substrates for supercapcitor application. Gurav et al prepared $Cu(OH)_2$ thin films by CBD method using $CuSO_4$ and ammonia as initial ingredients, for supercapacitor application [13]. Similarly, for other applications such as, catalysis and optoelectronic devices, $Cu(OH)_2$ thin films were reported by many scientists [14][15].

Based on above discussion, the present investigation reports on the synthesis of $Cu(OH)_2$ thin films by facile chemical bath deposition method. The structural, and morphological properties of $Cu(OH)_2$ thin films are reported here. Moreover, the electrochemical supercapacitor characteristics of $Cu(OH)_2$ films are investigated by using cyclic voltammetry and charge-discharge curves in 1 M KOH electrolyte. The supercapacitive performance were calculated and analyzed in terms of specific capacitance, specific energy and power density with electrochemical series resistance.

## II. EXPERIMENTAL DETAILS

For the growth of $Cu(OH)_2$ thin films a facile chemical bath deposition (CBD) method was used. In a typical synthesis, an aqueous solution of 50 mL containing (0.1 M) $Cu(NO_3)_2 \cdot 6H_2O$ and 0.1 M Urea ($CO(NH_2)_2$) was used under constant stirring. Stainless steel (SS) substrates were used for deposition, which were cleaned with detergent and rinsed with DI water along with further ultra-sonication for 10 min. The substrates were immersed in the prepared solution bath. The bath was sealed and placed in a vessel containing paraffin oil for constant heating and bath kept at 95°C temperature without stirring for 6 hours. During precipitation, a heterogeneous reaction occurred and Cu-based nanostructures were deposited on the substrates. The terminal thickness of 0.12 mg·$cm^{-2}$ was obtained after 6 h deposition. For further deposition (more than 6 h deposition time), decrease in film thickness observed, which could be attributed to the formation of outer porous layer and/or the film which may develop stress to cause delamination, resulting in peeling off the film after the film reaches at maximum thickness. After the 6 h reaction, thin film samples were cleaned by rinsing with DI water several times to remove the residual reactants. Then the samples were allowed to dry at room temperature and used as it is for further characterization.

The electrode materials were structurally characterized by XRD, XPS and FESEM measurements. The X-ray diffraction

(XRD) was carried out on a Rigaku Ultima diffractometer using

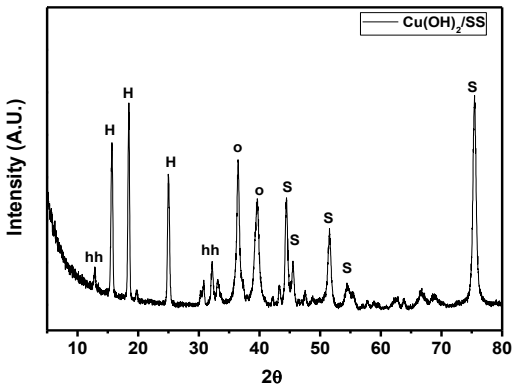


Fig. 1. XRD pattern of $Cu(OH)_2$/SS thin film

Cu-Kα radiation. X-ray photoelectron spectroscopy (XPS) measurements were carried out on a thermo scientific ESCALAB 250 (Thermo Fisher Scientific, UK). The morphology of the composite was examined by field-emission scanning electron microscopy (FESEM, JSM-7001F, JEOL). The supercapacitive performance was carried out by forming three electrode electrochemical system. The three electrode system consist of platinum (Pt) as counter electrode, MGF as a working electrode and Ag/AgCl as a reference electrode in 1 M KOH electrolyte. Cyclic Voltammetry (CV), galvanostatic charge/discharge tests and electrochemical impedance spectroscopy (EIS) were performed using ZIVE SP2 LAB analytical equipment (South Korea).

## III. RESULT AND DISCUSSION

### A. Film formation

Synthesis of $Cu(OH)_2$ on GF was achieved by using CBD method. CBD method is one of the efficient "bottom-up" approaches to grow nanostructures; it is based on the formation of a solid phase from solution which involves three collective steps as nucleation, coalescence and particle growth [16]. The greenish-blue $Cu(OH)_2$ thin films were prepared by chemical deposition method. The film growth is dominated by three periods: (i) an induction period (also called nucleation or incubation period) during which the various chemical equilibriums and reactions are established in the bath. The nuclei of the metal hydroxides formed on the substrate, (ii) the growth period during which the film thickness increases linearly with deposition time. The moment, the ionic product (IP) of the solution exceeds the solubility product (SP), and the solution reaches maximum degree of supersaturation (S = IP/SP), which consequently leads to the growth of nuclei and deposition of the film, and (iii) a terminal step where the reagent became depleted and film growth begins to slow down and eventually stops [13]. The possible reaction mechanism for the deposition of $Cu(OH)_2$ films is as follows:

In the formation $Cu(OH)_2$, as the temperature of solution bath increased to 95℃, decomposition of urea (reaction 1) took place, producing $CO_2$ and $NH_3$ gradually.

$$NH_2CONH_2 + H_2O \xrightarrow{\Delta} 2NH_3 + CO_2 \quad (1)$$

After decomposition of urea as per above reaction, the solution became alkaline, such an alkaline condition is more favorable to achieve supersaturation state, which is constructive to create more nucleation sites.

Simultaneously, $Cu^{2+}$ from $Cu(NO_3)_2 \cdot 6H_2O$ get mixed with $NH_3$ which formed amine complex. Such amine complexed metal ions easily get adsorbed on the heterogeneous surface of the substrate by electrostatic or Van-der Wall force. The specific surface area of substrate makes it easy to adsorb a large number of amine complexed $Cu^{2+}$.

$$Cu^{2+} + NH_3 \rightarrow Cu(NH_3)_4{}^{2+} \quad (2)$$

Initially, the solution was neutral with pH about ~6-7 and then increased gradually and monotonically with time and temperature, the solution became alkalescent. At this alkalescent bath condition, the $Cu(NH_3)_4{}^{2+}$ is instable and the following reactions occur to form mixed metal hydroxides on the SS surface in form of nano-buds.

$$Cu[(NH)_3]_4{}^{2+} + 2OH^1 \rightarrow Cu(OH)_2 + 4NH_3 \quad (3)$$

In the film formation $NH_3$, released from urea, introduced as a complexing agent in the bath and exerts itself to control the release velocity of $Cu^{2+}$ ions for deposition of $Cu(OH)_2$ nano-buds. After this reaction, lastly, green colored uniform film was found on the stainless steel substrate.

### B. Structural studies

The electrode materials were structurally characterized by XRD, XPS, Raman and FESEM measurements. The X-ray diffraction (XRD) was carried out on a Rigaku Ultima diffractometer using Cu-Kα radiation. The Fig. 1 shows X-ray diffraction (XRD) profiles of graphene foam and $Cu(OH)_2$/SS electrodes. Five significant diffraction peaks (2q) at ~45°, 46°, 51°,55° and 75° are attributed reflections of the crystalline peak of stainless steel substrate marked as 's'. The XRD pattern of $Cu(OH)_2$/SS electrode, which reveals characteristic peaks at ~13.3° (001), 30.8° (012), 31.9° (200) and 33.5° (11-2) belongs to the hydrated copper hydroxide ($Cu(OH)_2.nH_2O$) (JCPDS: 42-0638, marked as 'hh') with peaks at 16° (020), 18° (110) and 23° (021) attributed to $Cu(OH)_2$ (JCPDS 80-0656, marked as 'H') formation. Additionally, two peaks of Copper oxide (CuO) (JCPDS: 45-0937, marked as 'O') are found at 35.5° (002) and 38.7° (111). This results shows that, the formed film contains mixed phases of Copper oxide, hydroxide and hydrated hydroxide. Also, the good crystallinity of the deposited films of $Cu(OH)_2$ on SS can be assured by the high and sharper diffraction peaks.

To obtain more detailed information about elements and oxidation states of the prepared $Cu(OH)_2$/SS, X-ray photoelectron spectroscopy measurements were performed and corresponding results are presented in Fig. 2(a). Fig. 2(b) shows fitted spectra of Cu 2p for $Cu(OH)_2$/SS electrode. The Cu 2p spectrum was best fitted by considering two spin-orbit doublets and two shake-up satellites. Two kinds of copper species have

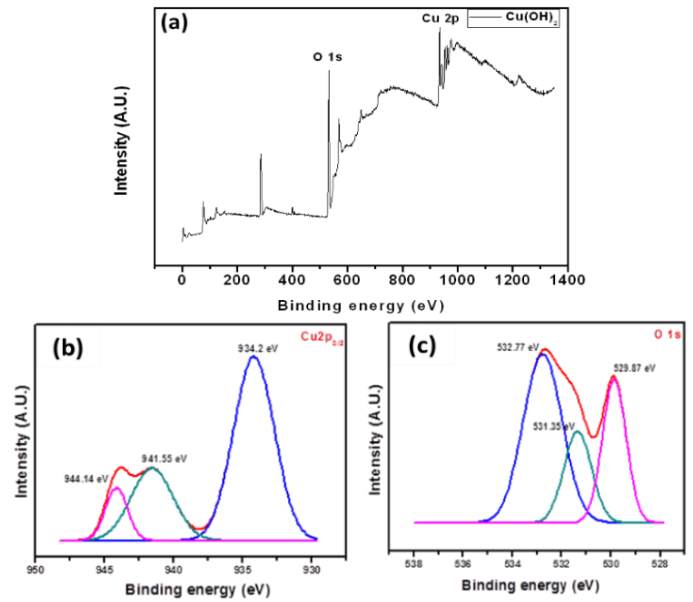


Fig. 2. (a) Full XPS spectra and core level. (b) Cu 2p. (c) O 1s spectra of $Cu(OH)_2$ thin film.

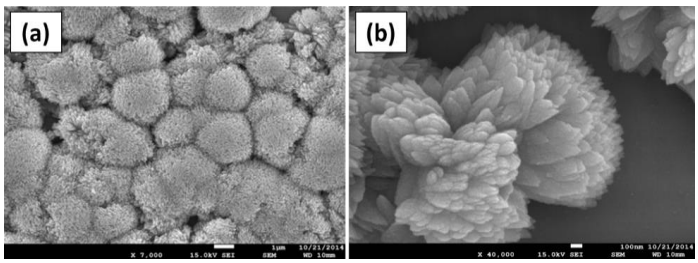


Fig. 3. FE-SEM images of $Cu(OH)_2$/SS at different (a) 7,000× and (b) 40,000× magnifications

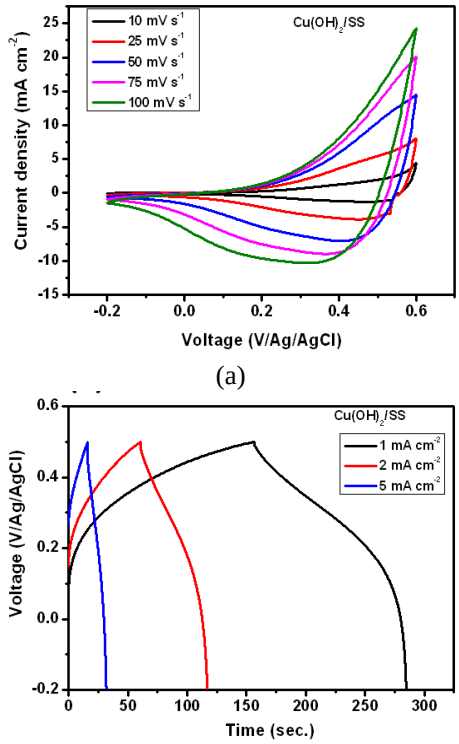


Fig. 4. Electrochemical studies of $Cu(OH)_2$/SS electrode. (a) CV curves of $Cu(OH)_2$/SS electrode in aqueous 1 M KOH at different scan rates (10-100 mV $s^{-1}$). (b) Galvanostatic charge-discharge (GCD) plots of $Cu(OH)_2$/SS electrode within potential window of -0.2 to 0.5 V at constant charging current from 1 to 5 mA $cm^{-2}$.

been detected and assigned to species containing $Cu^{2+}$ and $Cu^{3+}$ ions. Specifically, peak at binding energies (BE) of 934.2 eV can be ascribed to $Cu^{2+}$ while the peaks at BE of 941.5 and 944.1 eV are assigned to $Cu^{3+}$. According to the literature, the position of Cu (2p3/2) peak for $Cu(OH)_2$ chemical compositions is at binding energies of 934.2 eV [17]. To have detailed insight and the presence of hydroxide, O 1s core level of $Cu(OH)_2$ thin films was examined (Fig. 2(c)). The fitted spectrum for the O 1s region is shown in Fig. 2(c) reveals oxygen contributions in $Cu(OH)_2$/GF electrode. It is observed that the O1s core level region is composed of a broad peak centered at 532 eV for $Cu(OH)_2$ composition, which is associated with bound hydroxide groups ($OH^-$) and confirms the $Cu(OH)_2$ formation [18]. Thus, XPS studies support the formation of $Cu(OH)_2$ phase on SS substrate.

The surface morphology of the deposits was viewed by field-emission scanning electron microscopy (FESEM, JSM-7001F, JEOL). The FE-SEM micrographs of $Cu(OH)_2$/SS electrode at different magnifications are shown in Fig. 3(a-b). Fig.
3(a) shows that, $Cu(OH)_2$ film is nothing but formation of agglomerated micro sized flowers covering the entire surface of the SS substrate. Interestingly, a high magnification FESEM image (Fig. 3(b)) reveals that individual grain composed of several tiny nanoparticles aggregated into a nano-buds grain. The smaller nano-buds range from 50 to 75 nm in diameter. Such morphology offers higher surface area, which provides structural foundation for electrochemical processes. Highly oriented nano-bud-like microstructure is a potential candidate for supercapacitor application, provides large surface area; it possesses loosely packed structure and advantageous for the electrolyte ions to access the active materials, results in Faradaic reaction, which may contribute to enhancement of capacitive performance [19].

C. Supercapacitive study

Electrochemical performance was evaluated by testing by forming a conventional half-test cell, containing a three-electrode system with $Cu(OH)_2$ based nanostructured thin film as the working electrode, Ag/AgCl as reference electrode and platinum (Pt) as counter electrode in a 1 M KOH aqueous electrolyte. Cyclic voltammetry (CV), galvanostatic charge/discharge tests and EIS measurements were performed using ZIVE SP2 LAB analytical equipment (South Korea). The effect of scan rate on an electrochemical supercapacitor formed by $Cu(OH)_2$ was studied in 1 M KOH in the voltage range of -0.2 to 0.6 V and are presented in Fig. 4(a). The shape of the CV indicates that the capacitance characteristic is different from that of an electric double-layer capacitance in which the shape is normally close to an ideal rectangular shape. This finding suggests that the capacity results mainly from a pseudo-capacitive capacitance, which is based on a redox mechanism.

The appearance of anodic and cathodic peaks

corresponding to the $Cu(OH)_2$/CuOOH redox reaction in the CV is according to the following electrochemical reaction:

$$Cu(OH)_2 + OH^- \rightarrow CuOOH + H_2O + e^- \quad (4)$$

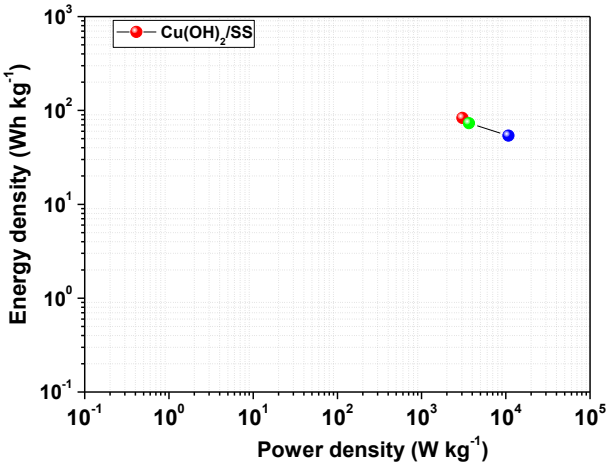


Fig. 5 Typical Ragone plot of energy density Vs power density

The redox peaks confirm the redox behavior of the synthesized product. The redox reaction of the copper electrode is usually considered to be a solid-to-solid transformation. The active material is thought to be a single-phase $Cu(OH)_2$, and the redox reaction involves the movement of protons and electrons into and out of the bulk of the solid phase. The area under the curve slowly increases with scan rate, this shows that, the voltammetric currents are directly proportional to the scan rate and thereby display capacitive behavior [20].

The Fig. 4 (b) shows the galvanostatic charge–discharge (GCD) of the $Cu(OH)_2$/SS at different constant current densities from 1 to 5 A $cm^{-2}$. The shape of the charge–discharge curves do not show the characteristic of a pure double-layer capacitor (linear charge-discharge), but mainly pseudocapacitance (non-linear charge-discharge), which corresponds with the result of the CV test [21]. The specific capacitance with different charge-discharge current density was calculated by using following formula.

$$C = \frac{I \times \Delta t}{V \times m} \quad (5)$$

where, '$I$' is the applied current density in ampere, '$\Delta t$' is discharging time, '$V$' is potential window and '$m$' is mass of active material. The specific capacitance was found to be ~340, 290 and 220 F $g^{-1}$ at 1, 2 and 5 mA $cm^{-2}$ current densities, respectively. The specific capacitance decreases with increase in charge-discharge current density. The decreasing specific capacitance is consequence of less active material access, which reduces the effective utilization of material at a higher charging-discharging rate. Maximum specific capacitance ~340 F $g^{-1}$ is observed for $Cu(OH)_2$/SS electrode at low charge-discharge current density at 1 mA $cm^{-2}$. Up to now, Dubal et al. [6] have obtained specific capacitance of 43 F $g^{-1}$ using CuO electrode prepared by high temperature chemical bath deposition method. Gurav et al. [13] have reported 120 F $g^{-1}$ supercapacitance of $Cu(OH)_2$ films prepared by CBD method using copper sulphate and ammonia as initial ingredients. Here, we obtained relatively high capacitance may be due to hydrous nature of $Cu(OH)_2$ electrode.

Furthermore, the specific energy (SE, Wh $kg^{-1}$), and the specific power (SP, kW $kg^{-1}$) calculated from the charge-discharge curve, using following equations (6, 7), respectively.

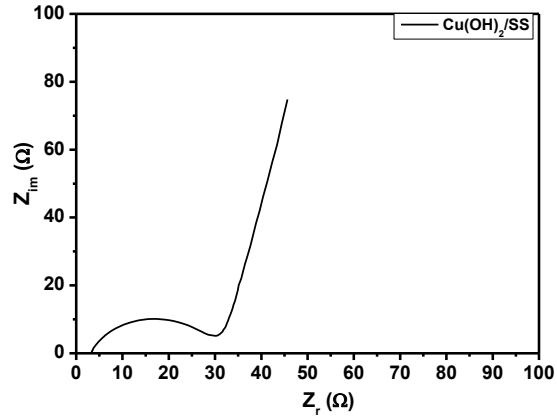


Fig. 6. Electrochemical impedance spectrum within 1 MHz to 10 mHz frequency region Nyquist plot of $Cu(OH)_2$/SS electrodes.

$$SE = \frac{1}{2} C_s V^2 \quad (6)$$

$$SP = \frac{SE}{\Delta t} \quad (7)$$

where, '$C_s$' is specific capacitance, '$V$' is operating potential window and '$\Delta t$' is discharging time. The calculated specific energy and power density from charge-discharge curves is shown in the typical Ragone plot (Fig. 5). The maximum energy density about 83 Wh $kg^{-1}$ at power density 3.1 kW $kg^{-1}$ observed for $Cu(OH)_2$/SS electrode, which is comparable with other metal oxides [21][22] and hydroxides [23]-[27].

To better understand the enormous benefit of the $Cu(OH)_2$ in supercapacitors, EIS measurements were employed at open circuit potential (OCP) over the frequency range of 1 MHz and 10 mHz for $Cu(OH)_2$/SS electrode and shown in Fig. 6. The complex-plane plot shown in Fig. 6 consists of a small semicircle at higher frequencies with a transition to a linear part at low frequencies. A sharp increase in '$Z_{im}$' at lower frequency is attributed to the capacitive behavior of the material. However, the semi-circle at higher frequencies implies charge transfer resistance ($R_{ct}$) at the electrode/electrolyte interface [21][28][29]. Apparently, the solution resistance ($R_s$) of the $Cu(OH)_2$/SS electrode (2.8 Ω) is much smaller, indicating a lower contact resistance. Along with negligible charge transfer resistance ($R_{ct}$) is observed for $Cu(OH)_2$/SS electrode (15.1 Ω) attributed to significant charge transfer and faster ion-transport behavior of composite electrode [28][29]. An impedance arc of a semicircle is visible in the high frequency region, attributed to the complicated interfaces at the $Cu(OH)_2$– $Cu(OH)_2$ nano-buds and $Cu(OH)_2$–substrate contacts since, electron hopping at these interfaces occurs during the charge/discharge processes [29]. This result signifies that the $Cu(OH)_2$ based electrode possesses lower contact and charge-transfer impedances. The porous $Cu(OH)_2$ nano-buds structure shortens ion diffusion paths and

facilitates migration of electrolyte ions at a large current density, as a result, ion diffusion and electron transfer accelerated at high cycling rates for the $Cu(OH)_2$/SS electrode.

This structural and electrochemical capacitive result signifies that, the $Cu(OH)_2$/SS electrode possesses good supercapacitor behavior. Also, the direct growth of $Cu(OH)_2$ by CBD method on SS avoids the addition of binder to attach nano-materials over metal-based current collector in traditional electrode fabrication process, which not only hamper the charge transport rate, but also increases the total mass of the electrode.

## IV. CONCLUSIONS

In summary, a CBD method was successfully employed for the deposition of $Cu(OH)_2$ microflowers consist of nano-buds onto SS surface. The structural analysis pattern revealed the polycrystalline and hydrous nature of the $Cu(OH)_2$ thin films. Formation of $Cu(OH)_2$ compound is also confirmed by XPS analysis. The FESEM images revealed the formation of microflowers of nano-buds covering the entire substrate surface area. The nano-bud like morphology of $Cu(OH)_2$ electrode reveals maximum specific capacitance up to ~340 F $g^{-1}$. This enhanced $Cu(OH)_2$/SS electrode performance open up further scope in symmetric, asymmetric, non-aqueous and solid state supercapacitive devices as per requirement of application (high energy or power). Thus, the facile CBD synthetic approach may provide a convenient route for the preparation of $Cu(OH)_2$/SS as efficient electrode in energy storage application.

## ACKNOWLEDGEMENT

This work was partially supported by a grant from R&D Program of the Korea Railroad Research Institute, the Yonsei University Future-leading Research Initiative of 2014 (2014-22-0168), the Pioneer Research Center Program (2010-0019313), the Priority Research Centers Program through the National Research Foundation of Korea (NRF) funded by the Ministry of Education, Science and Technology (2009-0093823), Basic Science Research Program through the National Research Foundation of Korea (NRF) grant funded by the Ministry of Education, Science and Technology (MEST) (2013-8-0874) and Korea Electric Power Corporation Research Institute though Korea Electrical Engineering & Science Research Institute (R14XA02-2).

## REFERENCES

[1] C.C. Hu, J.C. Chen, K.H. Chang, J. Power Sources, 221, (2013), 128–133.
[2] H. Zhang, Y. Wang, C. Liu, H. Jiang, J. Alloys Comp., 517, (2012), 1–8.
[3] C.D. Lokhande, A.M. More, J.L. Gunjakar, J. Alloys Comp., 486, (2009), 570–580.
[4] N. Li, M. Cao and C. Hu, Nanoscale, 4, (2012), 6205-6218.
[5] V.D. Patake, S.S. Joshi, C.D. Lokhande, O.S. Joo, Mater. Chem. Phys., 114, (2009), 6–9.
[6] D.P. Dubal, D.S. Dhawale, R.R. Salunkhe, V.S. Jamadade, C.D. Lokhande, J. Alloys Comp., 492, (2010), 26–30.
[7] J.S. Shaikh, R.C. Pawar, N.L. Tarwal, D.S. Patil, P.S. Patil, J. Alloys Comp., 509, (2011), 7168–7174.
[8] D. Kim, K.Y. Rhee, S.J. Park, J. Alloys Comp., 530, (2012), 6–10.
[9] S. Kandalkar, J. Gunjakar and C. Lokhande, Appl. Surf. Sci., 254, (2008), 5540-5544.
[10] I.L. Zhang, Z. Xiong, X.S. Zhao, J. Power Sources, 222, (2013), 326–332.
[11] P. Gao, M. Zhang, Z. Niu, Q. Xiao, Chem. Commun., 48, (2007), 5197–5199.
[12] L. Zhu, Y. Chen, Y. Zheng, N. Li, J. Zhao, Y. Sun, Mater. Lett., 64, (2010), 976–979.
[13] K.V. Gurav, U.M. Patil, S.W. Shin, G.L. Agawane, M.P. Suryawanshi, S.M. Pawar, P.S. Patil, C.D. Lokhande, J.H. Kim, J. Alloys Comp., 509, (2011), 27–31.
[14] X. Liu, Z. Li, Q. Zhang, F. Li, T. Kong, Mater. Lett., 72, (2012), 49–52.
[15] X. Guan, L. Li, G. Li, Z. Fu, J. Zheng, T. Yan, J. Alloys Comp., 509, (2011), 3367–3374.
[16] G. Hodes, Phys. Chem. Chem. Phys., 9, (2007), 2181-2196.
[17] C. Zhu, A. Oshero and Matthew J. Panzer, Electrochimica Acta, 111, (2013), 771-778.
[18] F. Wang, W. Tao, M. Zhao, M. Xu, S. Yang, Z. Sun, L. Wang, J. Alloys Comp., 509, (2011), 9783–9803.
[19] S. B. Kulkarni, U. M. Patil, I. Shackery, J. S. Sohn, S. Lee, B. Park and S. Jun, J. Mater. Chem. A, 2, (2014), 4989-4998.
[20] U.M. Patil, K.V. Gurav, V.J. Fulari, C.D. Lokhande, O.S. Joo, J. Power Sources, 188, (2009), 338–342.
[21] U.M. Patil, S.B. Kulkarni, V.S. Jamadade, C.D. Lokhande, J. Alloys Comp., 509, (2011), 1677–1682.
[22] A. Bruke, J. Power Sources, 91, (2000), 37-50.
[23] U.M. Patil, Su Chan Lee, J.S. Sohn, S.B. Kulkarni, K.V. Gurav, J.H. Kim, Jae Hun Kim, Seok Lee, Seong Chan Jun, Electrochimica Acta, 129, (2014), 334–342.
[24] U. M. Patil, M. S. Nam, J. S. Sohn, S. B. Kulkarni, R. Shin, S. Kang, S. Lee, J. H. Kim and S. Chan Jun, J. Mater. Chem. A, 2, (2014), 19075-19083.
[25] J. Chen, J. Xu, S. Zhou, N. Zhao and C.-P. Wong, J. Mater. Chem. A, 3, (2015), 17385-17391.
[26] A. Pramanik, S. Maiti and S. Mahanty, Dalton Trans., 44, (2015), 14604-14612.
[27] S.K. Shinde, D.P. Dubal, G.S. Ghodake, D.Y. Kim, V.J. Fulari, Journal of Electroanalytical Chemistry, 732, (2014), 80–85.
[28] C.-C. Hu, W.-C. Chen, Electrochimica Acta, 49, (2004), 3469–3477.
[29] V. Ganesh, S. Pitchumani, V. Lakshminarayanan, Journal of Power Sources, 158, (2006), 1523–1532.